Supporting Information

Nanosphere [Ag(SR)]$_n$: Coordination polymers of Ag$^+$ with a combination of a hydrophilic and a hydrophobic thiols

Yan Xu, Su-Li Dong, Xiao-Sheng Yan, Qian Wang, Zhao Li and Yun-Bao Jiang*

Department of Chemistry, College of Chemistry and Chemical Engineering, the MOE Key Laboratory of Spectrochemical Analysis and Instrumentation, and iChEM, Xiamen University, Xiamen 361005, China

E-mail: ybjiang@xmu.edu.cn

Electronic Supplementary Information (ESI)

CONTENTS

1. Experimental Section

Materials. All of the chemicals are commercially available and used without further purification. Silver nitrate (AgNO$_3$, >98%) was purchased from Sangon (Shanghai, China), Silver triflate (CAgF$_3$O$_3$S, 98%), Silver hexafluoroantimonate (AgSbF$_6$, 97%), Silver tetrafluoroborate (AgBF$_4$, 99%), L-cysteine (L-Cys, >99%), D-cysteine (D-Cys, 99%), L-Homocysteine (L-Hcys, >98%), Glutathione (GSH, >98%), D-penicillamine (D-Pen, >99%), N-Acetyl-L-cysteine (NAcCys, >98%), *n*-butyl mercaptan (*n*-BuSH, >99%) and other mercaptans (*n*-C$_n$H$_{2n+1}$SH)were purchased from Energy Chemical (Shanghai, China). Other chemicals (AR) were obtained from Guoyao (Shanghai, China).

Characterization. Absorption spectra were recorded on a Thermo Evolution 300 absorption spectrophotometer using a 1-cm quartz cell. CD spectra were recorded on a Jasco-810 CD spectrometer. Dynamic light scattering (DLS) measurements were performed on a Malvern Zetasizer Nano ZS. ^{1}H NMR spectra were recorded on Ascend III-850 spectrometer. High-resolution transmission electron microscopy (TEM, JEM-2100) images were taken at an accelerating voltage of 200 kV. AFM images were taken on the Cypher S facility.

Experimental Procedures. Ag$^+$-(Cys+*Bu*SH) solution was prepared by added Cys (25 μL, 2 mM) and *Bu*SH (2.5 μL, 20 mM) to 2 mL 10 mM pH 5.0 HAc-NaAc buffer solution. Then Ag$^+$ (1.4 μL, 50 mM) was added by titrating. The mixed solution was recorded timely by absorption spectra and CD spectra.

(Ag$^+$-Cys)-*Bu*SH solution was prepared by mixing Cys (25 μL, 2 mM) and Ag$^+$ (1.0 μL, 50 mM) in 2 mL 10 mM pH 5.0 HAc-NaAc buffer solution to form Ag$^+$-Cys polymers first. Then *Bu*SH (2.5 μL, 20 mM) was added to the Ag$^+$-Cys solution. The mixed solution was recorded timely by absorption spectra and CD spectra.

(Ag$^+$-*Bu*SH)-Cys solution was prepared by mixing *Bu*SH (2.5 μL, 20 mM) and Ag$^+$ (1.0 μL, 50 mM) in 2 mL 10 mM pH 5.0 HAc-NaAc buffer solution to form Ag$^+$-*Bu*SH polymers first. Then Cys (25 μL, 2 mM) was added to the Ag$^+$-*Bu*SH solution. The mixed solution was recorded timely by CD spectra.

The TEM samples were prepared by depositing a drop (10 μL) of the prepared sample solution onto a carbon-coated copper grid. A piece of filter paper was employed to remove the excess solution on the grid, and then the grid was allowed to dry under vacuum conditions.

The AFM samples were prepared by depositing a drop (10 μL) of the prepared sample solution onto silicon wafer interface and dried under vacuum ambient conditions. Because the size of the probe was much larger than the diameter of the nanosphere polymer (TEM), the

width measured by such probes appears much larger than it was, and the height information was used to determine the height of the nanosphere structure from side view.

2. Supplementary Spectral Data
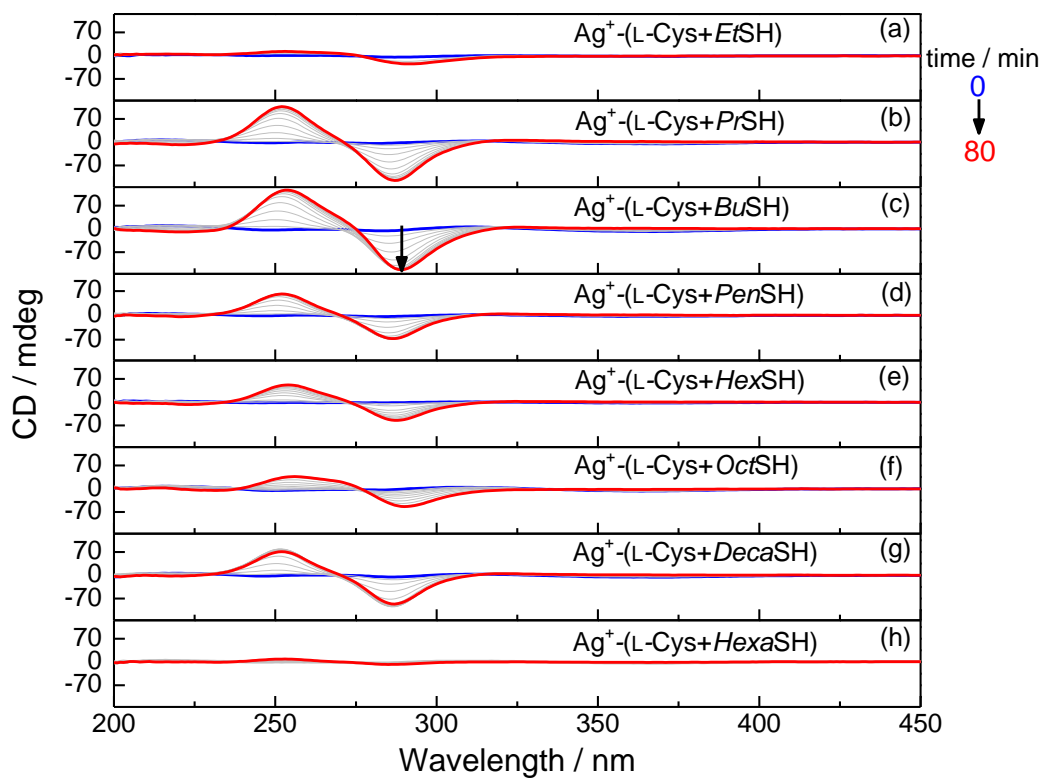
Fig. S1 Time evolution of CD spectra of Ag^+-(L-Cys+n-$C_nH_{2n+1}SH$) in 10 mM pH 5.0 HAc-NaAc solution. [L-Cys] = [n-$C_nH_{2n+1}SH$] = 25 μM, [Ag^+] = 35 μM, time = 0 - 80 min.
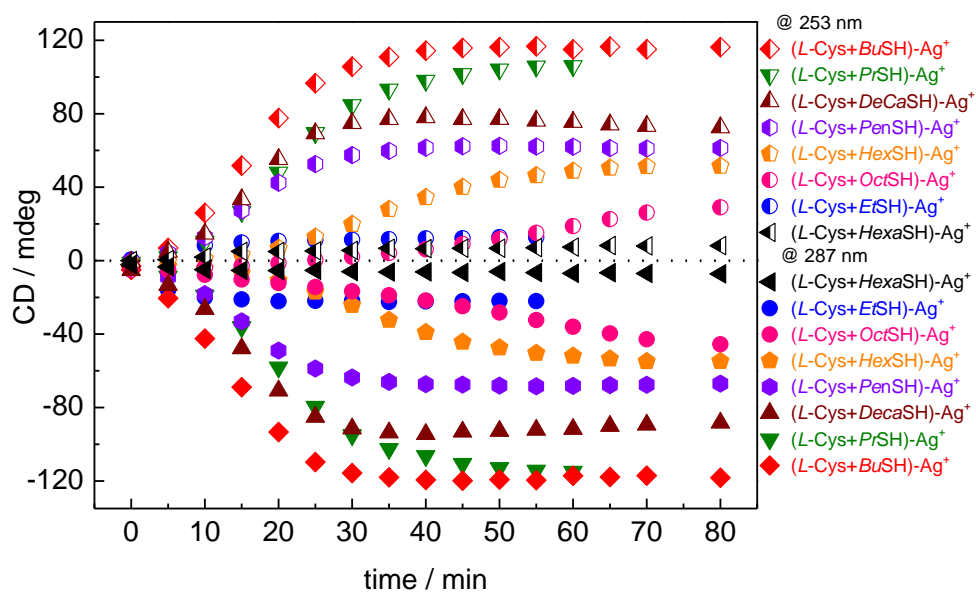
Fig. S2 Time dependent CD signals of Ag^+-(L-Cys+n-$C_nH_{2n+1}SH$) system in 10 mM pH 5.0 HAc-NaAc solutions. [L-Cys] = [n-$C_nH_{2n+1}SH$] = 25 μM, [Ag^+] = 35 μM, time = 0 - 80 min.
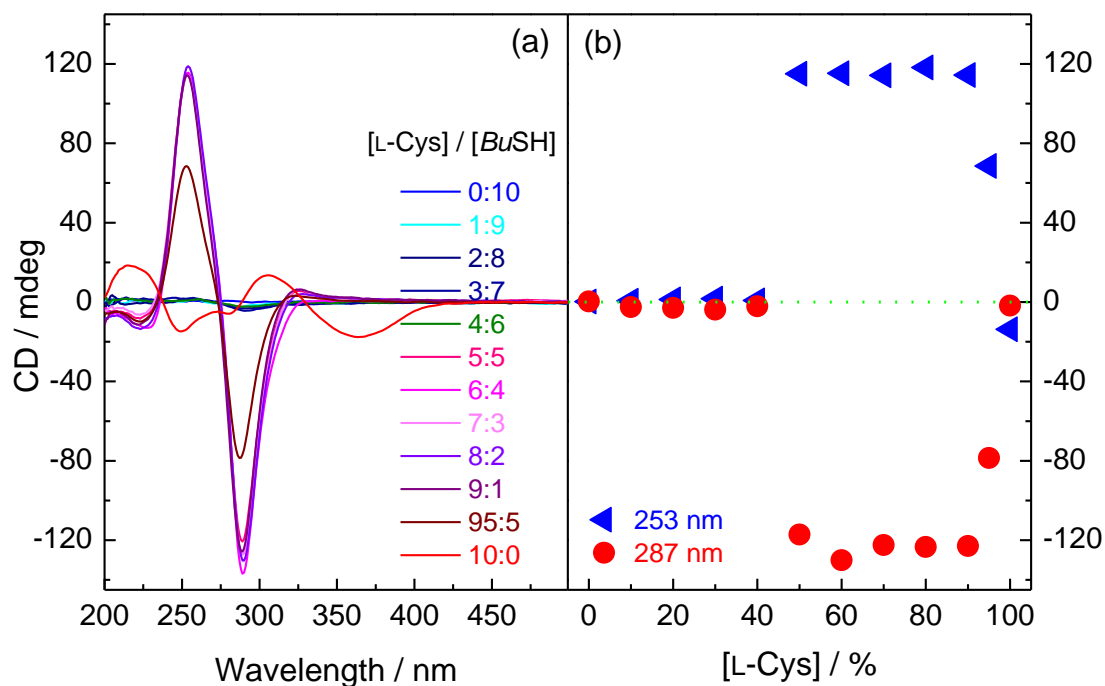
Fig. S3 CD spectra (a) and plots of CD signals at 253 nm and 287 nm (b) of Ag^+-(L-Cys+BuSH) as a function of molar fraction of L-cysteine in the total thiol ligands in 10 mM pH 5.0 HAc-NaAc solution. [L-Cys] + [BuSH] = 50 μM, [Ag^+] = 35 μM, mixing time = 80 min.
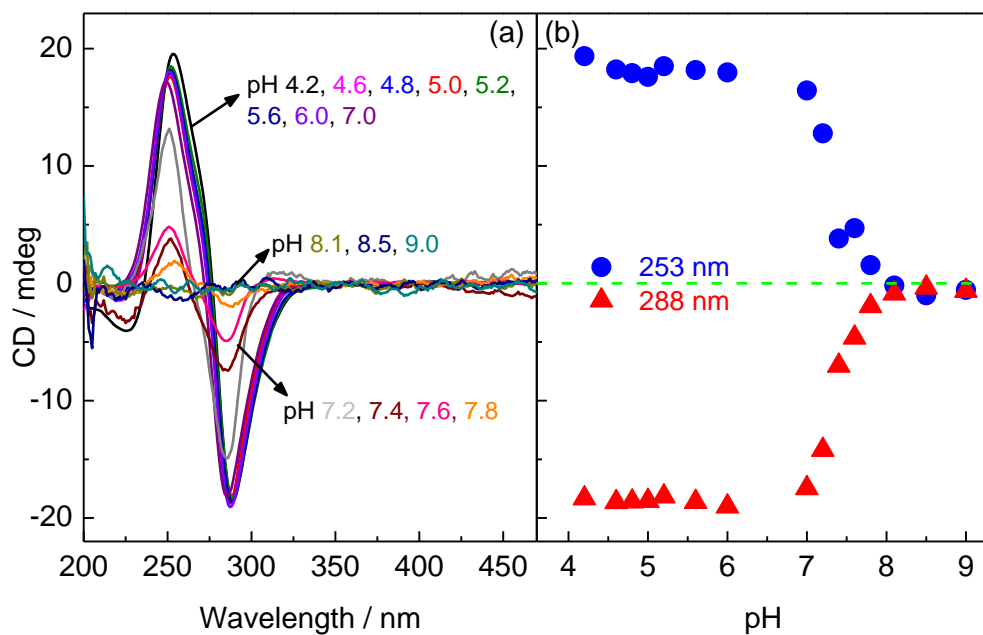
Fig. S4 CD spectra (a) and plots of CD spectra (b) of Ag$^+$-(L-Cys+*Bu*SH) solutions of varing pH values. [L-Cys] = [*Bu*SH] = 2.5 μM, [Ag$^+$] = 3.5 μM, time = 80 min.
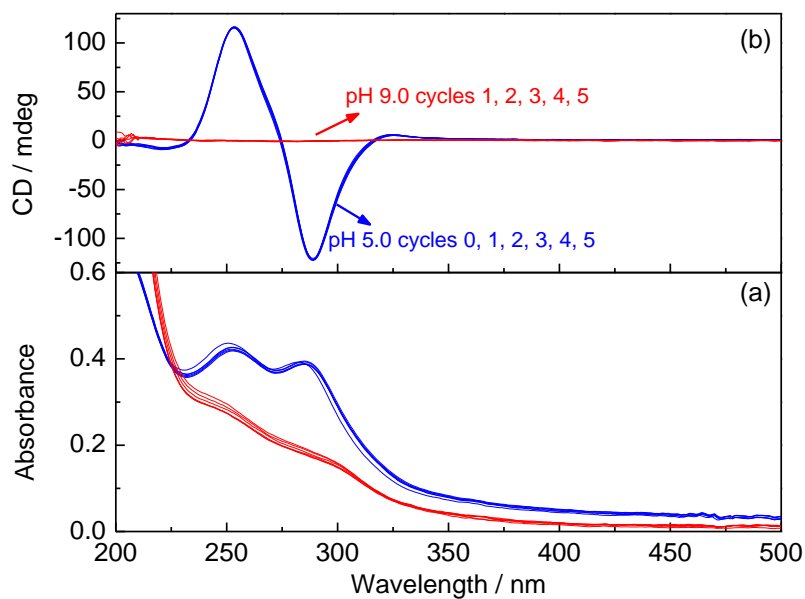
Fig. S5 Absorption (a) and CD spectra (b) of Ag$^+$-(L-Cys+*Bu*SH) solution as pH was switched between 5.0 and 9.0. [L-Cys] = [*Bu*SH] = 25 μM, [Ag$^+$] = 35 μM, time = 80 min.
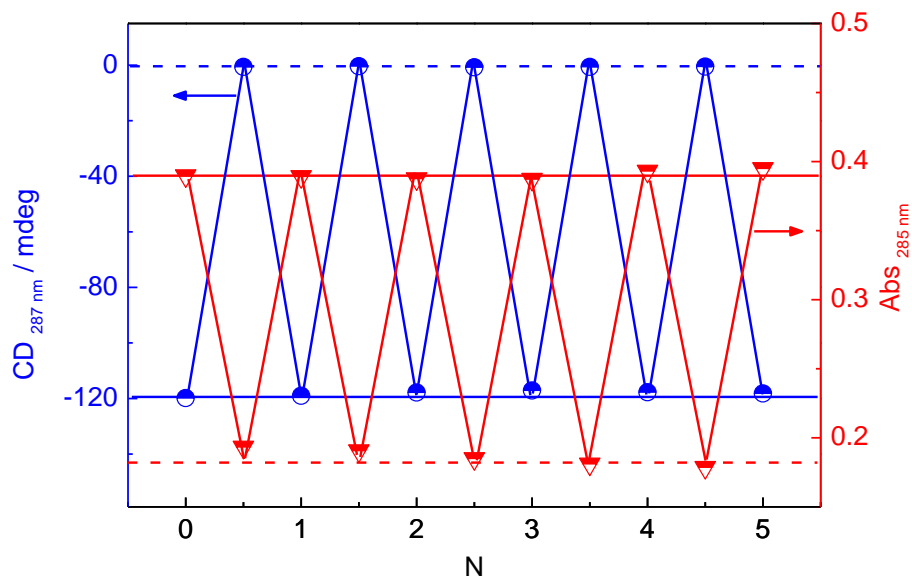
Fig. S6 Evolution of CD ellipticity (blue) and absorbance of Ag⁺-(L-Cys+*Bu*SH) solution as solution pH was switched between 5.0 and 9.0. [L-Cys] = [*Bu*SH] = 25 μM, [Ag⁺] = 35 μM, time = 80 min.
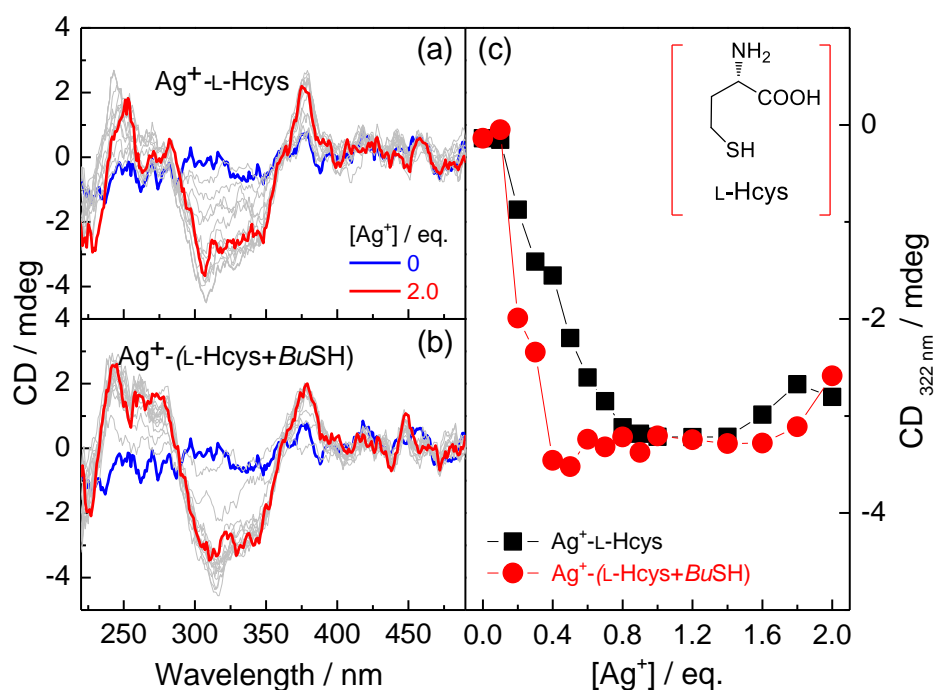
Fig. S7 CD spectra of Ag⁺-L-Hcys (a) and Ag⁺-(L-Hcys+*Bu*SH) (b), and plots of CD signal at 322 nm versus concentration of Ag⁺ (c) in 10 mM pH 5.0 HAc-NaAc solution. [L-Hcys] = [*Bu*SH] = 25 μM, [Ag⁺] = 0 - 2.0 eq.
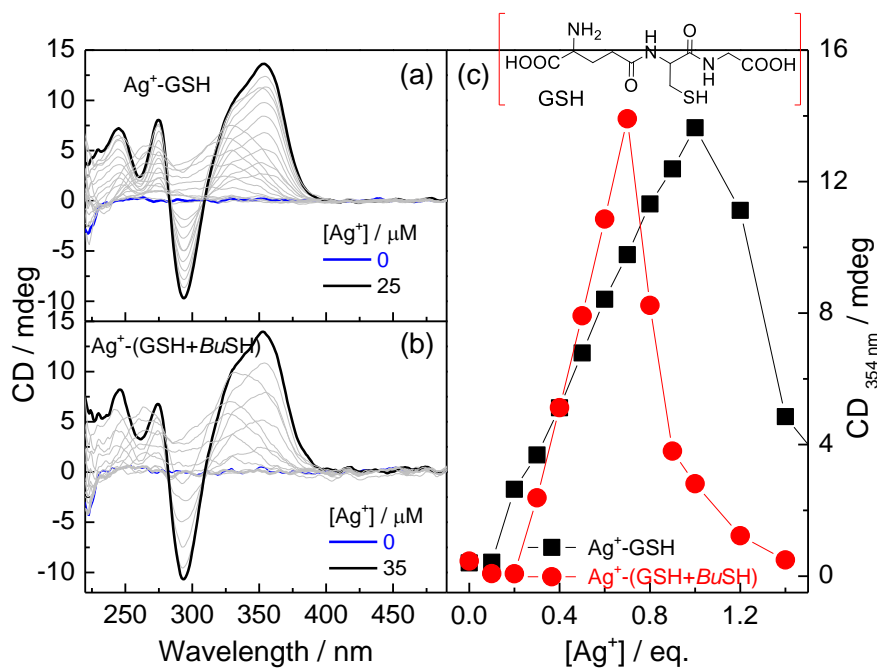
Fig. S8 CD spectra of a) Ag$^+$-GSH and b) Ag$^+$-(GSH+BuSH) and c) plots of CD signal at 354 nm versus concentration of Ag$^+$ in 10 mM pH 3.8 HAc-NaAc buffer. [GSH] = [BuSH] = 25 μM, [Ag$^+$] = 0 - 70 μM.
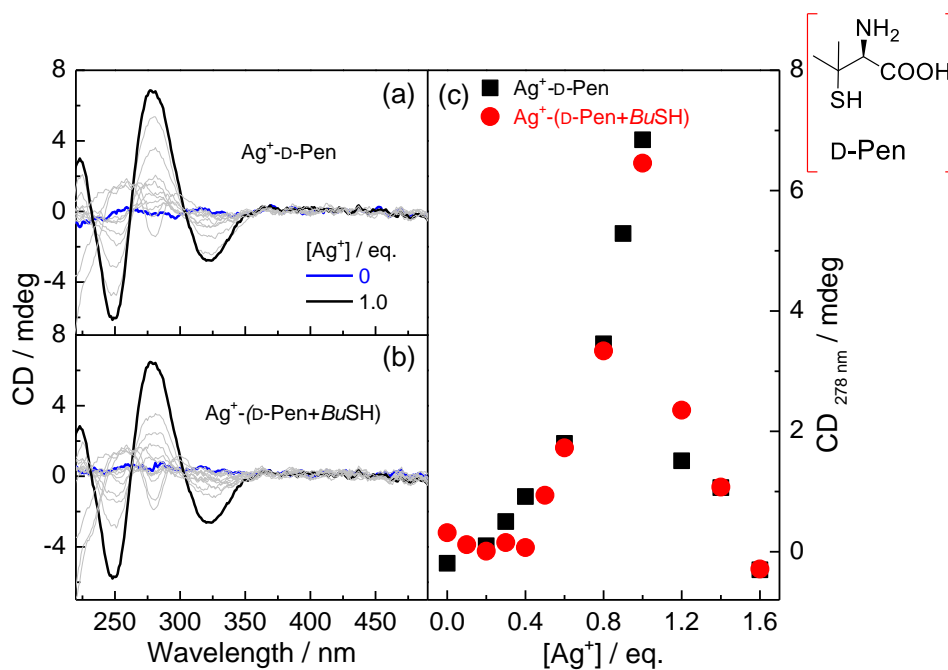
Fig. S9 CD spectra of Ag$^+$-D-Pen (a) and Ag$^+$-(D-Pen+BuSH) (b) and plots of CD signal at 278 nm versus concentration of Ag$^+$ (c) in 10 mM pH 5.0 HAc-NaAc buffer. [D-Pen] = [BuSH] = 25 μM, [Ag$^+$] = 0 -1.6eq.
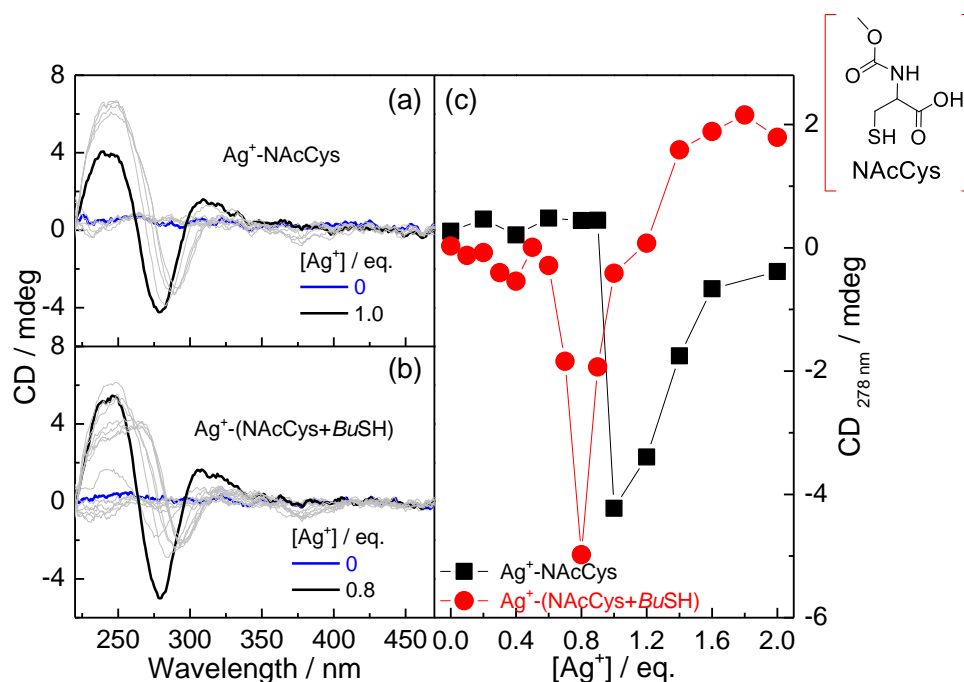
Fig. S10 CD spectra of Ag$^+$-NAcCys (a) and Ag$^+$-(NAcCys+BuSH) (b), and plots of CD signal at 278 nm versus concentration of Ag$^+$ (c) in 10 mM pH 5.0 HAc-NaAc solution. [NAcCys] = [BuSH] = 25 μM, [Ag$^+$] = 0 -2.0 eq.
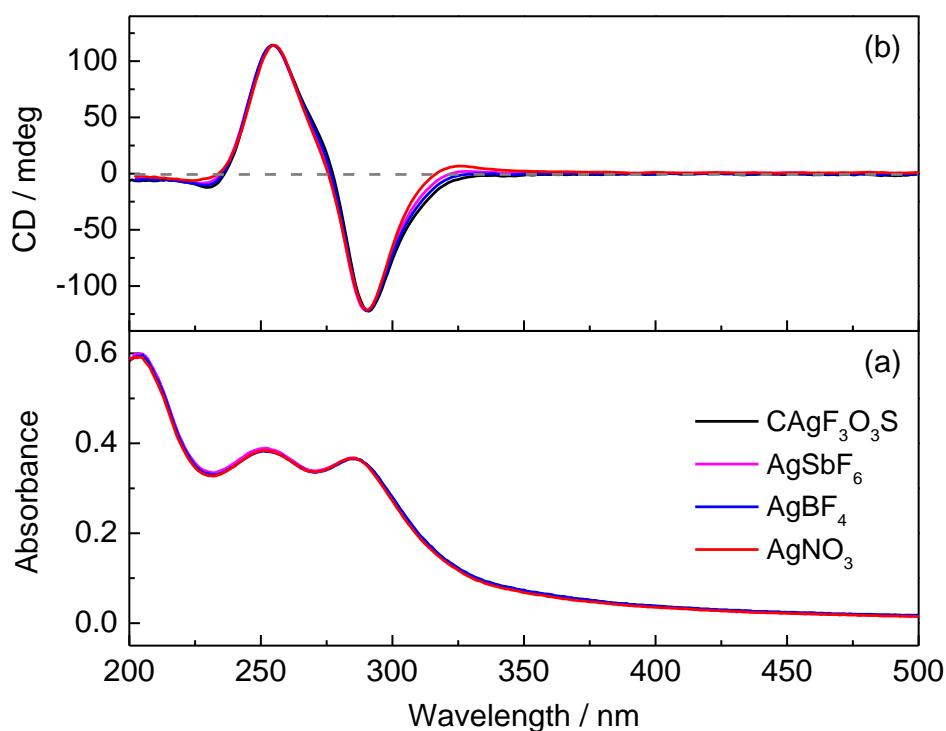
Fig. S11 Absorption (a) and CD (b) spectra of Ag$^+$-(L-Cys+BuSH) with varying counter anions in 10 mM pH 5.0 HAc-NaAc buffer. [L-Cys] = [BuSH] = 25 μM, [CAgF$_3$O$_3$S] = [AgSbF$_6$] = [AgBF$_4$] = [AgNO$_3$] = 35 μM, time = 80 min.
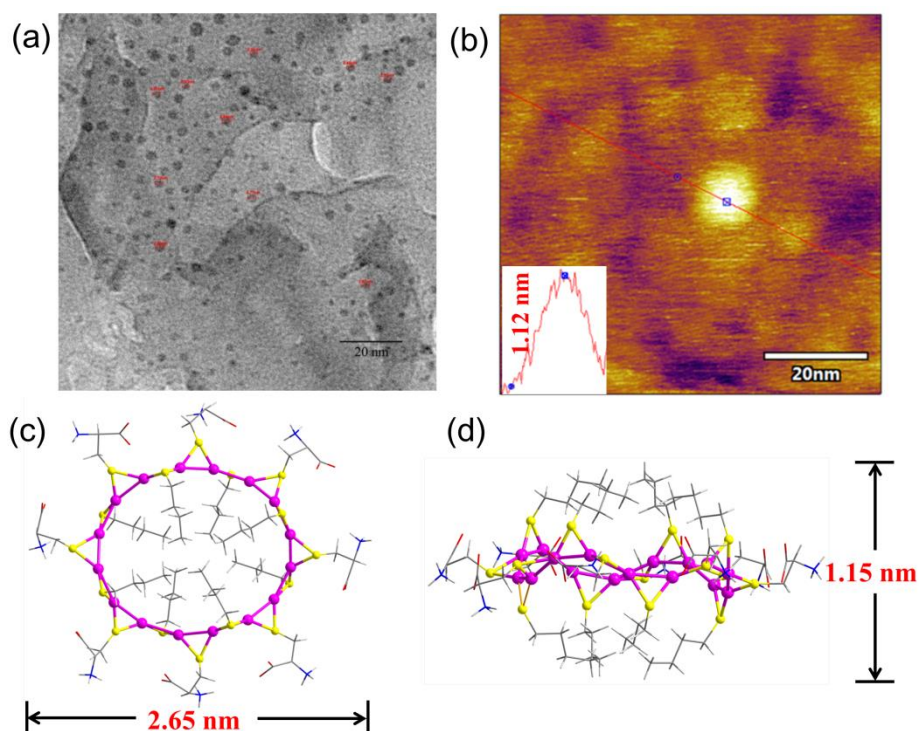
Fig. S12 (a) High-magnification TEM image of Ag$^+$-(Cys+*Bu*SH) polymers and (b) AFM image of Ag$^+$-(Cys+*Bu*SH) polymers at the silicon wafer interface and height profile along the red line. (c) Width of Ag$^+$-(Cys+*Bu*SH) polymer based on the structural model from top view shown in Scheme 1b using Gaussian modeling and (d) height of Ag$^+$-(Cys+*Bu*SH) polymer based on the structural model from side view shown in Scheme 1b using Gaussian modeling. The structure was drawn by using Gaussian structural modelling without further optimization.
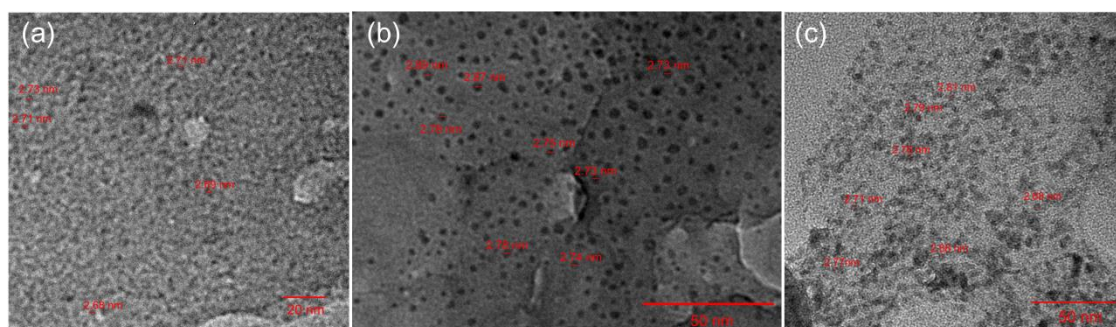
Fig. S13 High-magnification TEM image of Ag$^+$-(Cys+*Bu*SH) polymers varying the concentration of total thoil ligands (a-c). [Cys] + [*Bu*SH] = 2 μM (a), 5 μM (b), and 10 μM (c), [Ag$^+$] = 0.7 eq.
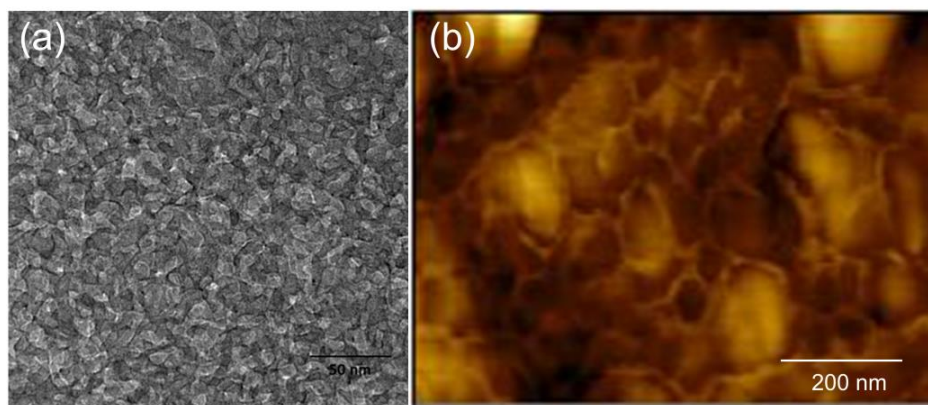
Fig. S14 High-magnification TEM (a) and AFM (b) images of Ag$^+$-L-Cys polymers.
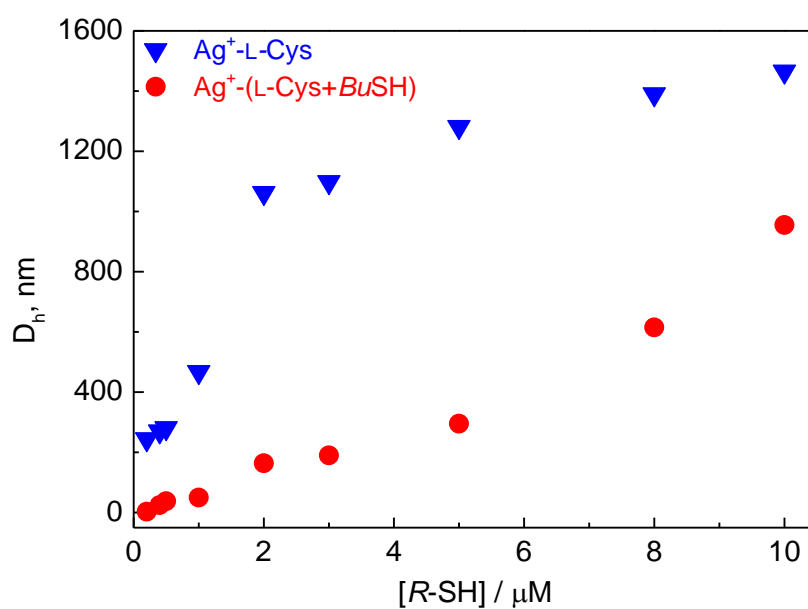
Fig. S15 DLS measured hydrodynamic diameters (D$_h$) of Ag$^+$-(L-Cys+BuSH) and Ag$^+$-L-Cys coordination polymers of varying concentration in 10 mM pH 5.0 HAc-NaAc buffer solution. [R-SH] = 0.2, 0.4, 0.5, 1.0, 2.0, 3.0, 5.0, 8.0, 10.0 μM, [Ag$^+$] = 1.0 eq.
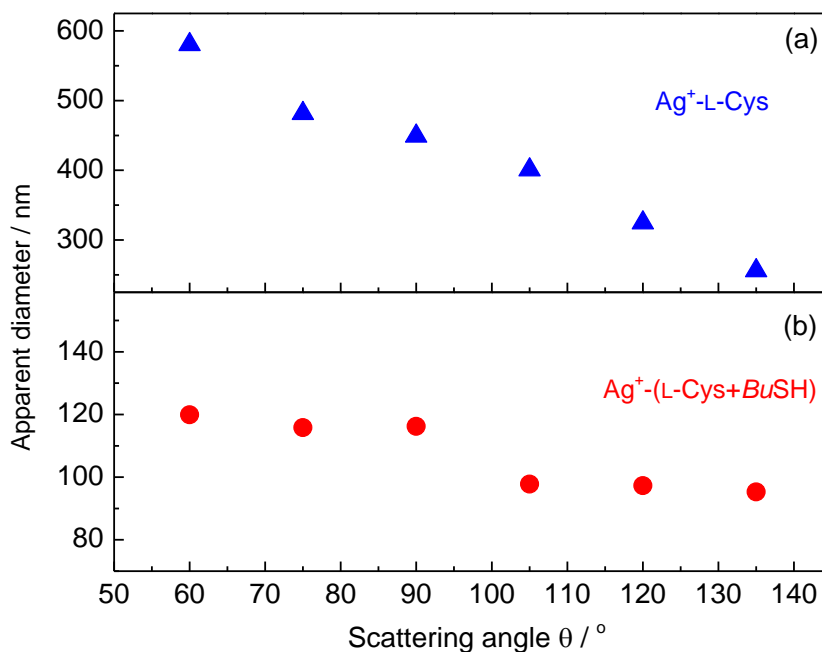
Fig. S16 Apparent hydrodynamic diameters of Ag$^+$-L-Cys (a) and Ag$^+$-(L-Cys+*Bu*SH) (b) solutions measured at different scattering angles θ at 25 °C. [L-Cys] = 1 μM, [Ag$^+$] = 1.0 μM (a); [L-Cys] = [*Bu*SH] = 0.75 μM, [Ag$^+$] = 1.5 μM (b). For species of isotropic or quasi-isotropic shape, such as spherical or quasi-spherical clusters, the diameters are invariant or weakly fluctant at different scattering angles.[1] The conventional hydrodynamic diameters are measured at a fix angle of 90°. The hydrodynamic diameters of Ag$^+$-L-Cys solutions measured at different scattering angles varied significantly, suggesting a pronounced anisotropy of the polymeric species that is indicative of the chain-like polymer structure (a). The hydrodynamic diameters of Ag$^+$-(L-Cys+*Bu*SH) solutions are however weakly fluctuant with scattering angles, in consistent with the nanosphere structures (b).
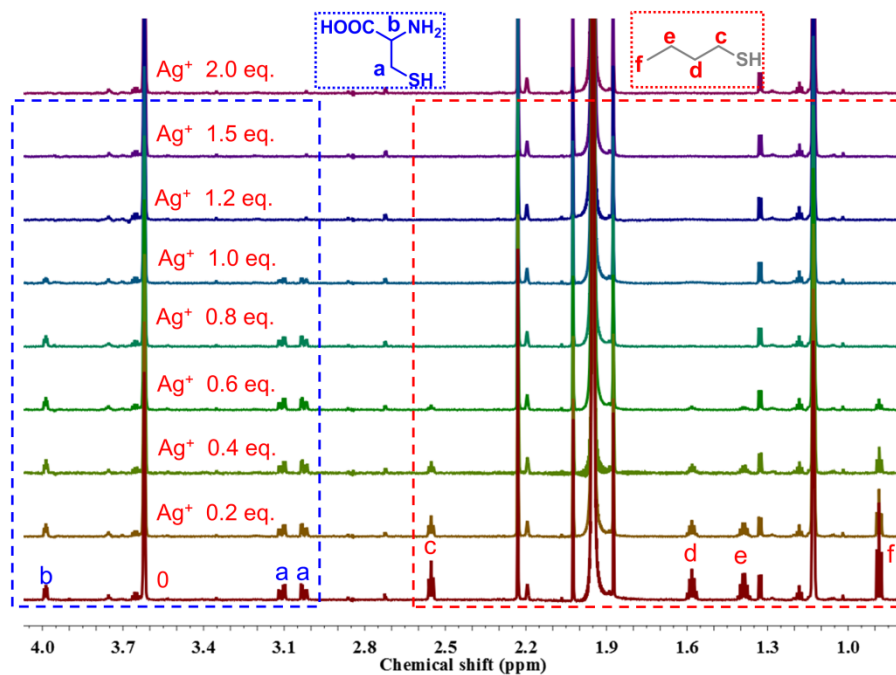
Fig. S17 Partial ^{1}H NMR spectra of L-Cys and *Bu*SH in the presence of Ag$^+$ in Ag$^+$-(L-Cys+*Bu*SH) system in 10 mM pH 5.0 HAc-NaAc D$_2$O solution using acetone as an internal standard. [L-Cys] = [*Bu*SH] = 50 µM, [Ag$^+$] = 0 - 200 µM.
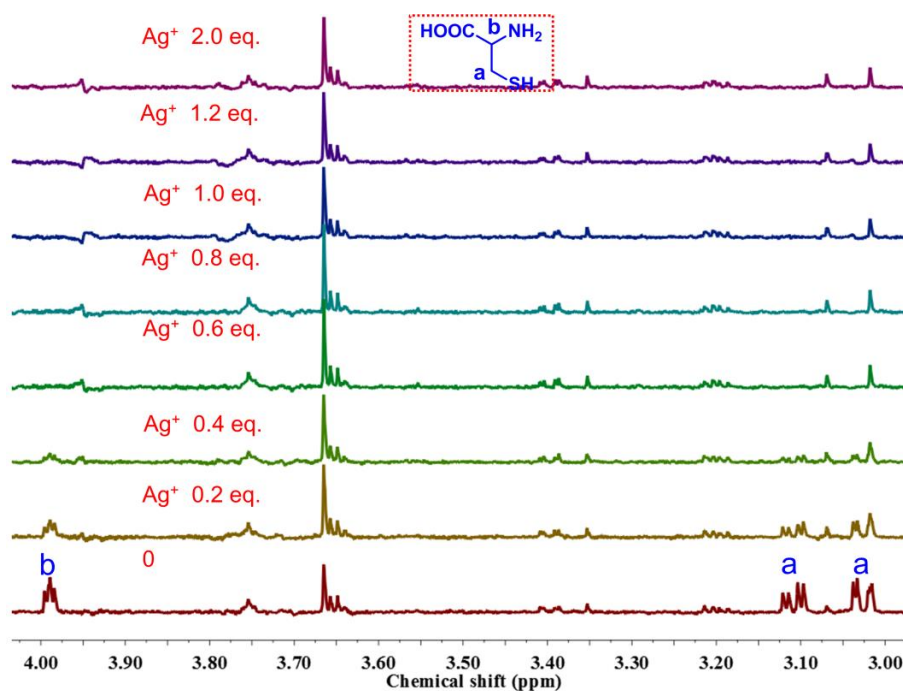
Fig. S18 Partial ^{1}H NMR spectra Ag$^+$-L-Cys in 10 mM pH 5.0 HAc-NaAc D$_2$O solution using acetone as an internal standard. [L-Cys] = 50 µM, [Ag$^+$] = 0 - 100 µM.
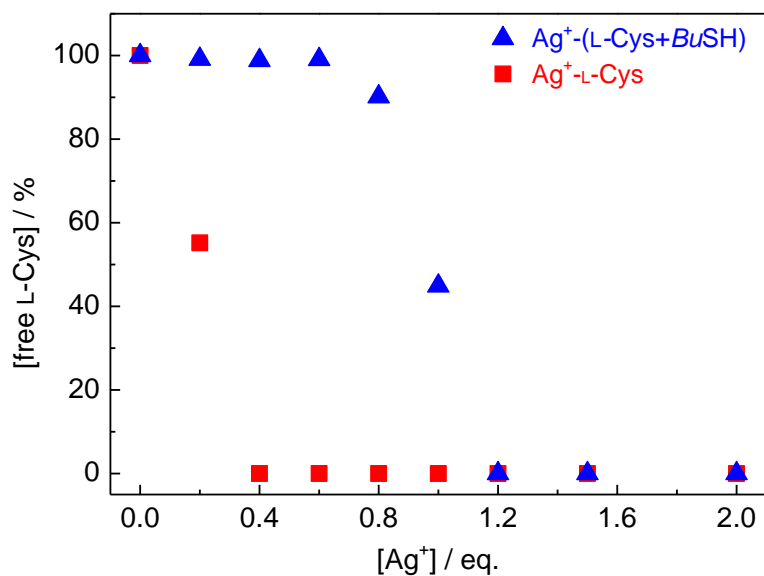
Fig. S19 Content of free L-Cys revealed by ^{1}H NMR versus equivalent of added Ag$^+$ in Ag$^+$-(L-Cys+*Bu*SH) and Ag$^+$-L-Cys system. [*Bu*SH] = 50 μM, [L-Cys] = 50 μM, [Ag$^+$] = 0 - 2.0 eq.
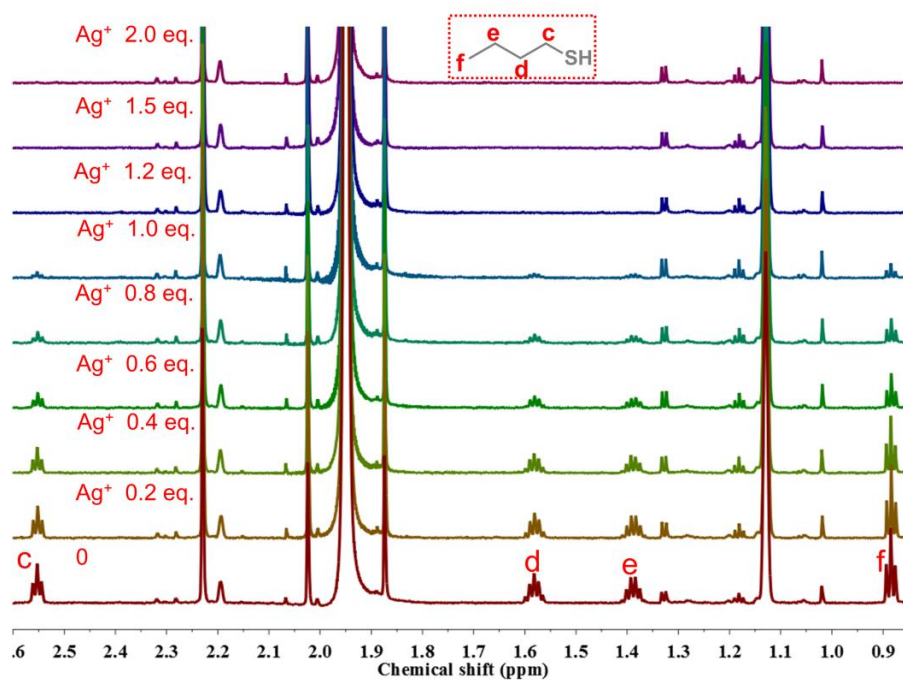
Fig. S20 Partial ^{1}H NMR spectra of Ag$^+$-*Bu*SH in 10 mM pH 5.0 HAc-NaAc D$_2$O solution using acetone as an internal standard. [*Bu*SH] = 50 μM, [Ag$^+$] = 0 - 100 μM.
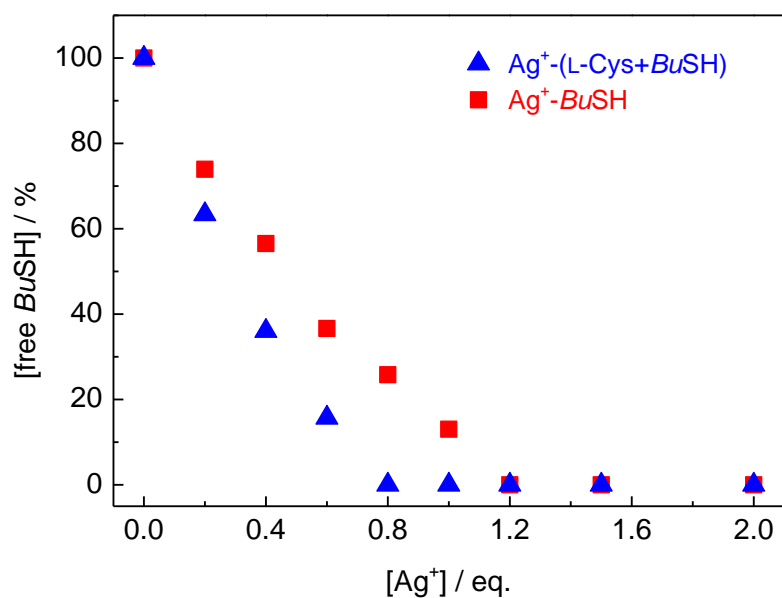
Fig. S21 Content of free *Bu*SH revealed by ^{1}H NMR versus equivalent of added Ag+ in Ag+-(L-Cys+*Bu*SH) and Ag+-*Bu*SH system. [*Bu*SH] = 50 μM, [L-Cys] = 50 μM, [Ag+] = 0 - 2.0 eq.
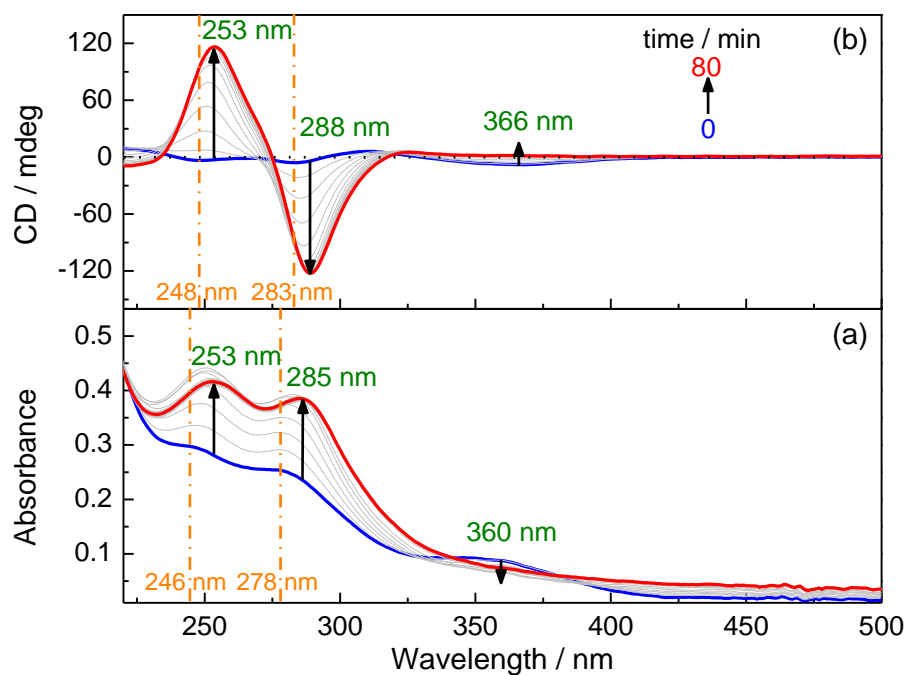
Fig. S22 Time evolution of absorption (a) and CD (b) spectra of Ag+-(L-Cys+*Bu*SH) in 10 mM pH 5.0 HAc-NaAc buffer. [L-Cys] = [*Bu*SH] = 25 μM, [Ag+] = 35 μM, time = 0 - 80 min.
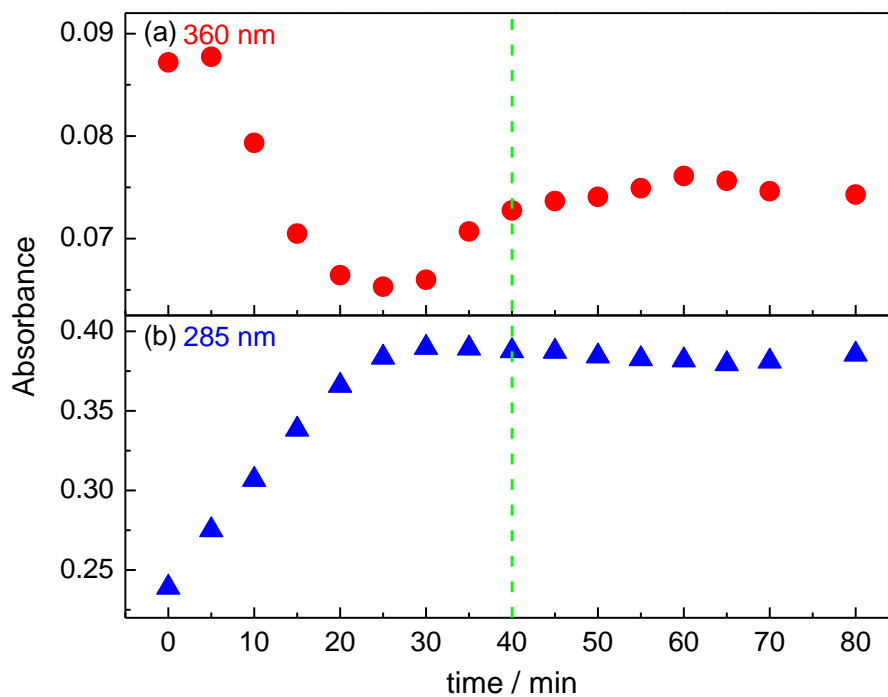
Fig. S23 Time profiles of absorbance at 360 nm (a) and 285 nm (b) of Ag$^+$-(L-Cys+BuSH) in 10 mM pH 5.0 HAc-NaAc solution. [L-Cys] = [BuSH] = 25 μM, [Ag$^+$] = 35 μM, time = 0 - 80 min.
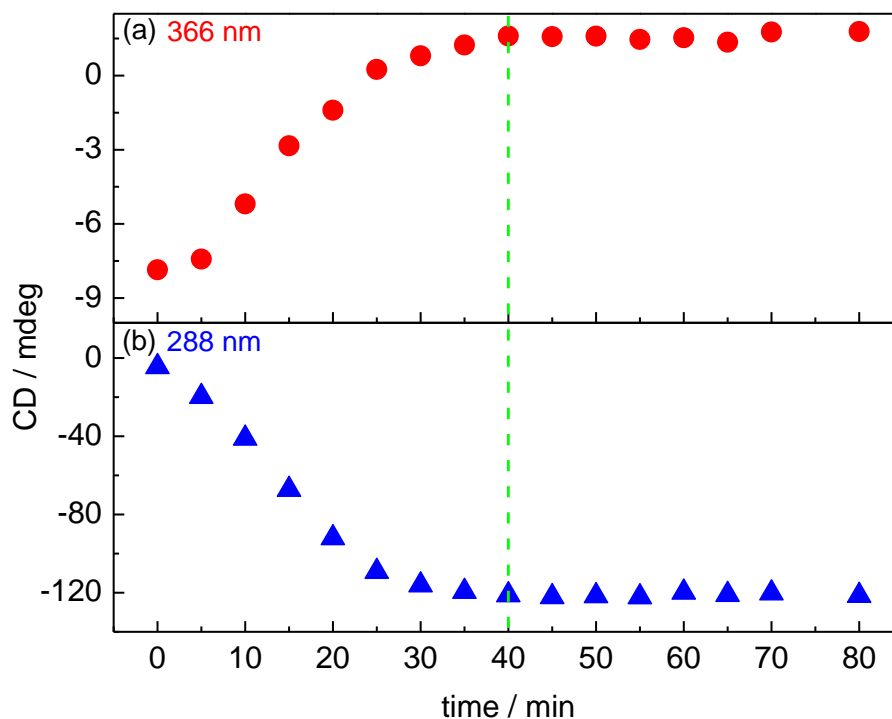
Fig. S24 Time profiles of CD signals at 366 nm (a) and 288 (b) of Ag$^+$-(L-Cys+BuSH) in 10 mM pH 5.0 HAc-NaAc solution. [L-Cys] = [BuSH] = 25 μM, [Ag$^+$] = 35 μM, time = 0 - 80 min.
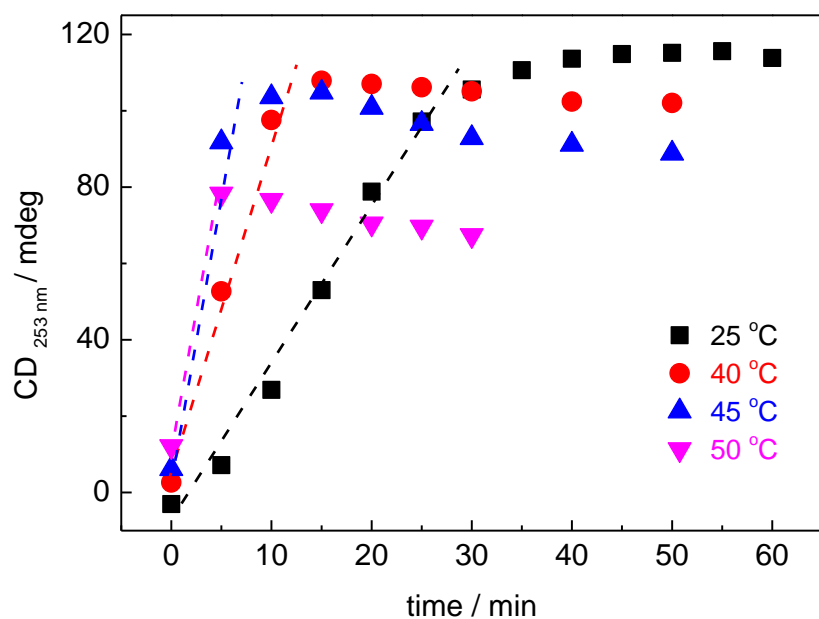
Fig. S25 Time evolution of the CD signal at 253 nm of Ag^+-(L-Cys+BuSH) in 10 mM pH 5.0 HAc-NaAc solution at 25, 40, 45 and 50 °C. [L-Cys] = [BuSH] = 25 μM, [Ag^+] = 35 μM, time = 0 - 60 min.
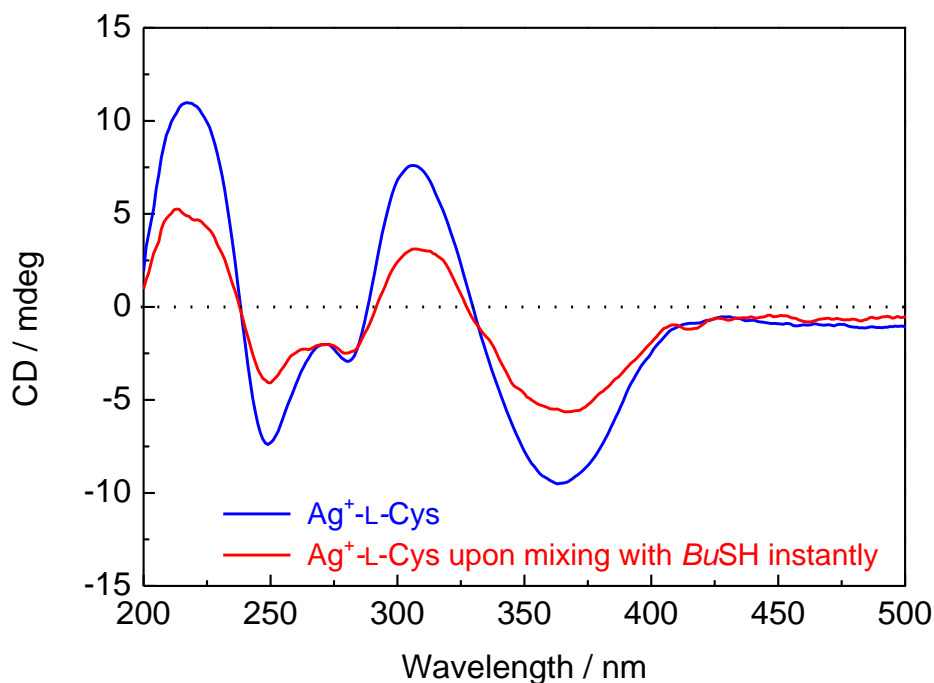
Fig. S26 CD spectra of Ag^+-L-Cys (blue line) and of Ag^+-L-Cys upon mixing with BuSH (red line) in 10 mM pH 5.0 HAc-NaAc buffer. [L-Cys] = [Ag^+] = 25 μM, [BuSH] = 25 μM.
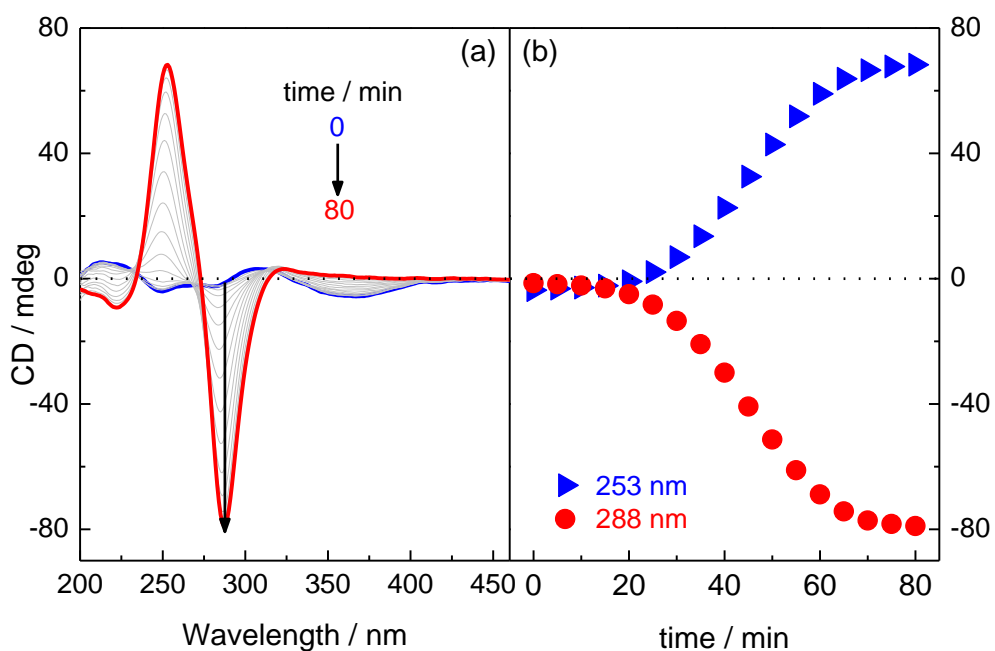
Fig. S27 Time traces of CD spectra (a) and profiles of CD signals (b) of Ag⁺-L-Cys system after adding *Bu*SH in 10mM pH 5.0 HAc-NaAc buffer solution. [L-Cys] = [Ag⁺] = 25 μM, [*Bu*SH] = 25 μM, time = 0 - 80 min.
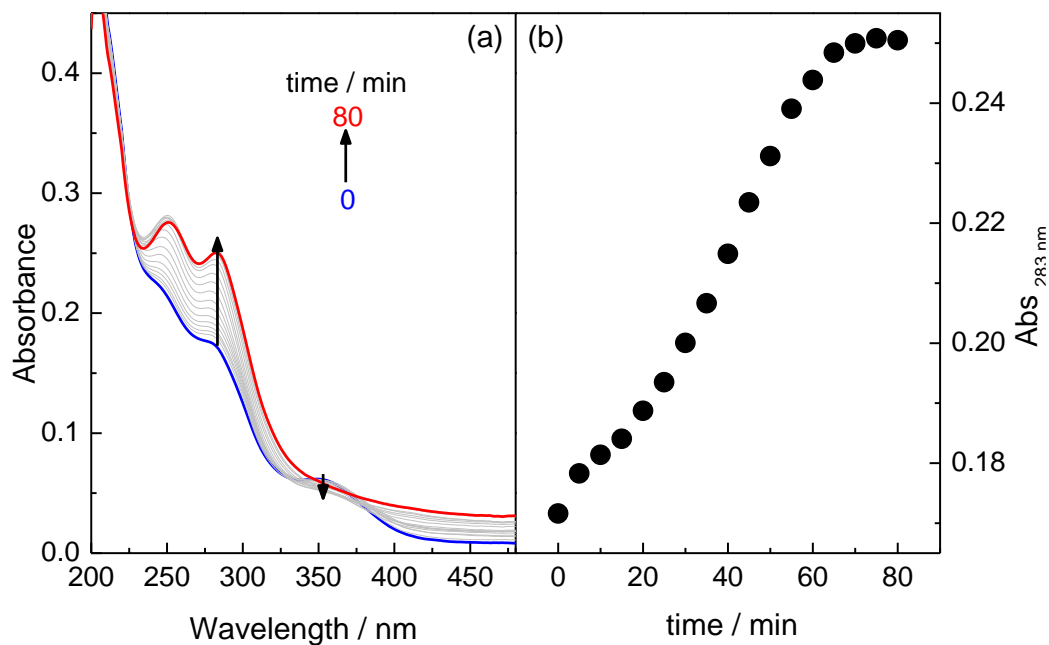
Fig. S28 Time traces of absorption spectra (a) and profile of absorbance at 283 nm (b) of Ag⁺-L-Cys system after adding *Bu*SH in 10 mM pH 5.0 HAc-NaAc buffer solution. [L-Cys] = [Ag⁺] = 25 μM, [*Bu*SH] = 25 μM, time = 0 - 80 min.
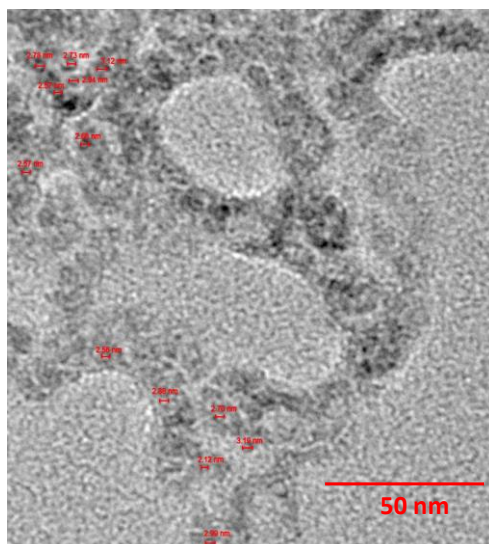
Fig. S29 TEM image of L-Cys-Ag⁺-*Bu*SH solution 80 minutes after mixing. The sample was prepared by dropping the solution onto carbon-coated copper grids followed by solvent evaporation in vacuum. [L-Cys] = [Ag⁺] = 5 μM, [*Bu*SH] = 5 μM.
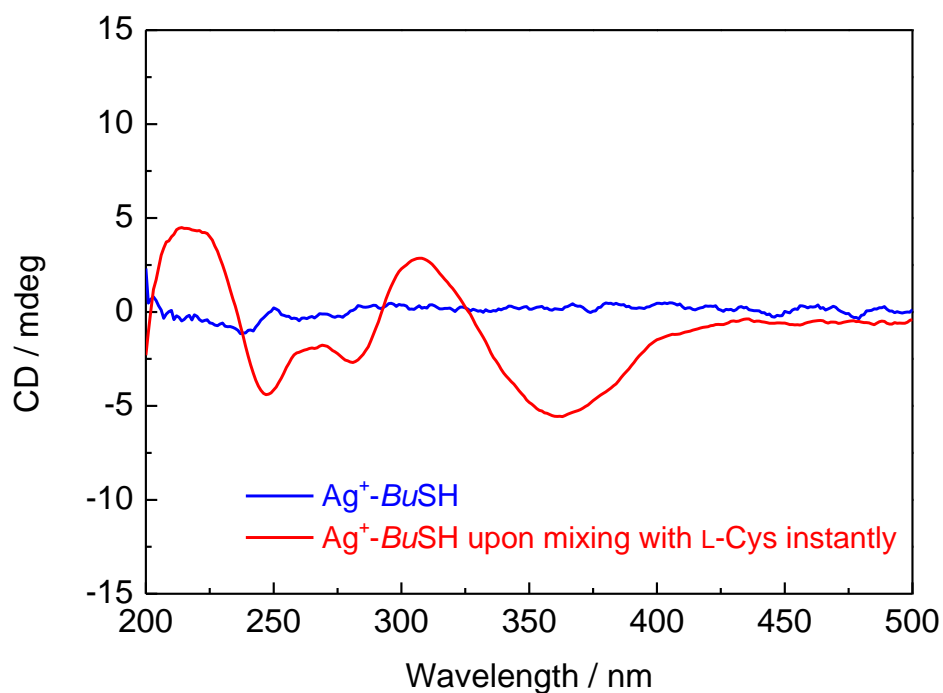
Fig. S30 CD spectra of Ag⁺-*Bu*SH (blue line) and Ag⁺-*Bu*SH system upon mixing with L-Cys (red line) in 10 mM pH 5.0 HAc-NaAc buffer solution. [*Bu*SH] = [Ag⁺] = 25 μM, [L-Cys] = 25 μM.
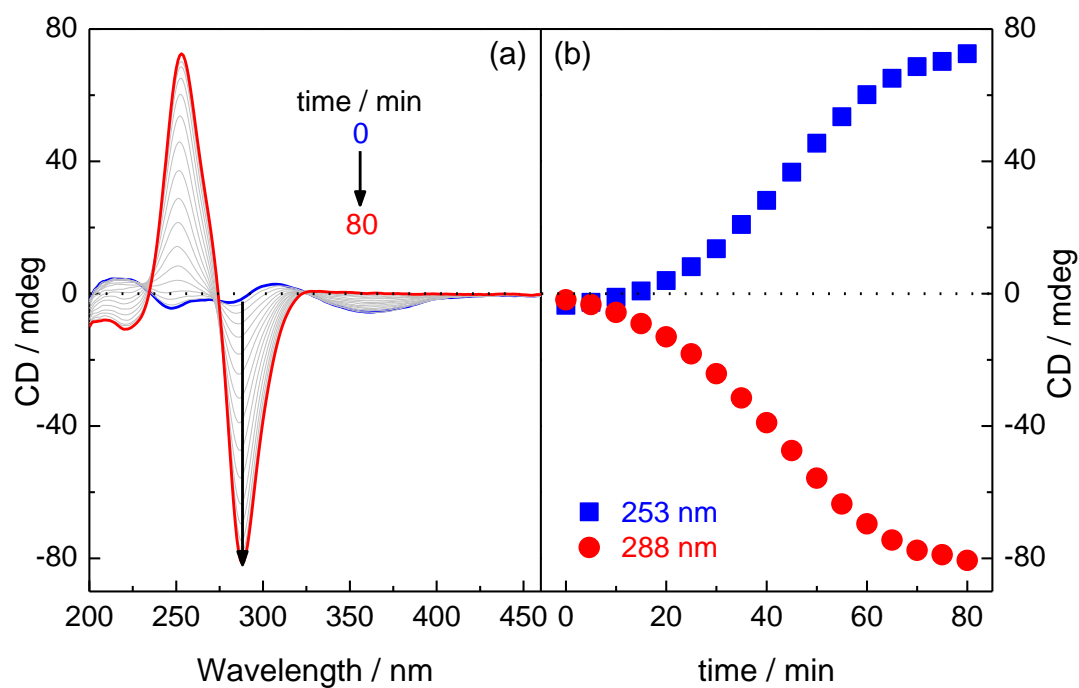
Fig. S31 Time profiles of CD spectra (a) and CD signals (b) of Ag$^+$-*Bu*SH system after adding L-Cys in 10 mM pH 5.0 HAc-NaAc buffer solution. [*Bu*SH] = [Ag$^+$] = 25 μM, [L-Cys] = 25 μM, time = 0 - 80 min.
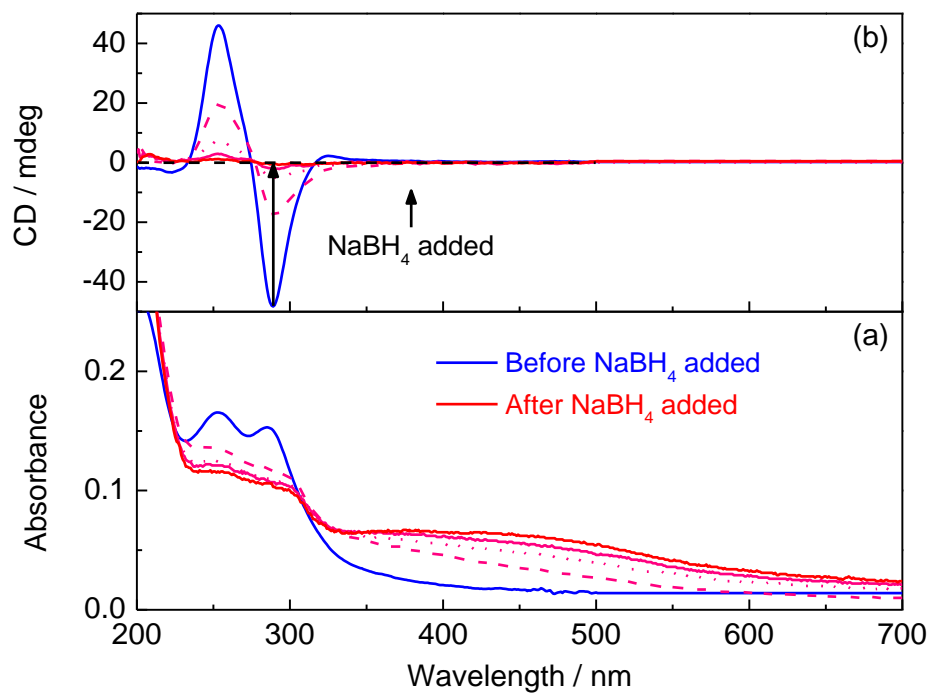
Fig. S32 Absorption (a) and CD spectra (b) of Ag$^+$-(L-Cys+*Bu*SH) in 10 mM pH 5.0 HAc-NaAc buffer solution upon reduction by NaBH$_4$ of increased duration. [L-Cys] = [*Bu*SH] = 10 μM, [Ag$^+$] = 14 μM, [NaBH$_4$] = 0 - 160 μM.
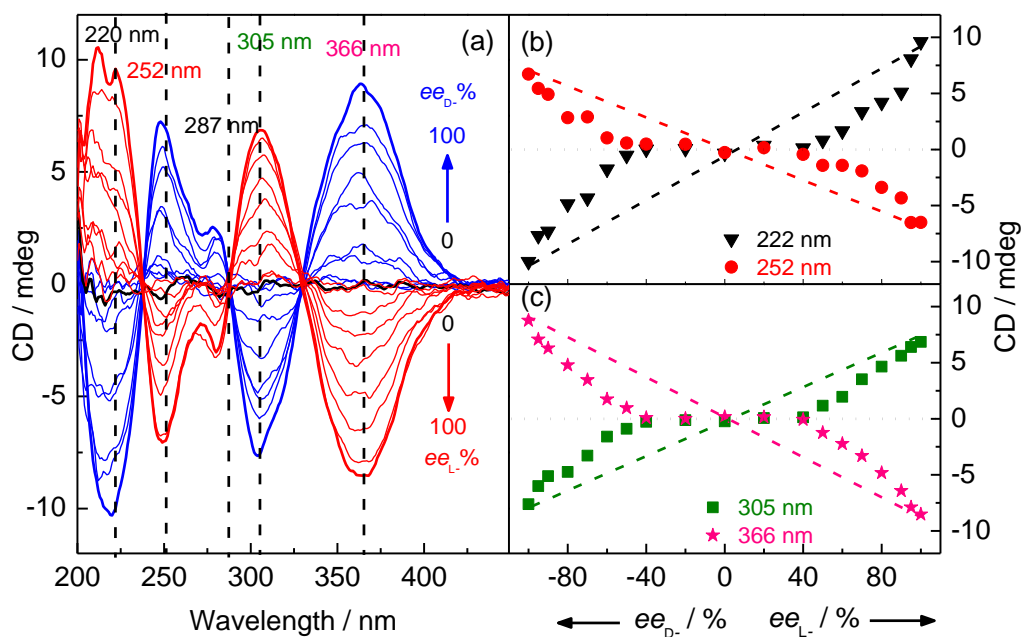
Fig. S33 CD spectra (a) and plots of CD signals at 222 nm and 252 nm (b) and at 305 nm and 366 nm (c) of Ag$^+$-Cys with varying *ee* of cysteine in 10 mM HAc-NaAc buffer of pH 5.0. [Ag$^+$] = 25 μM, [D-Cys] + [L-Cys] = 25 μM.
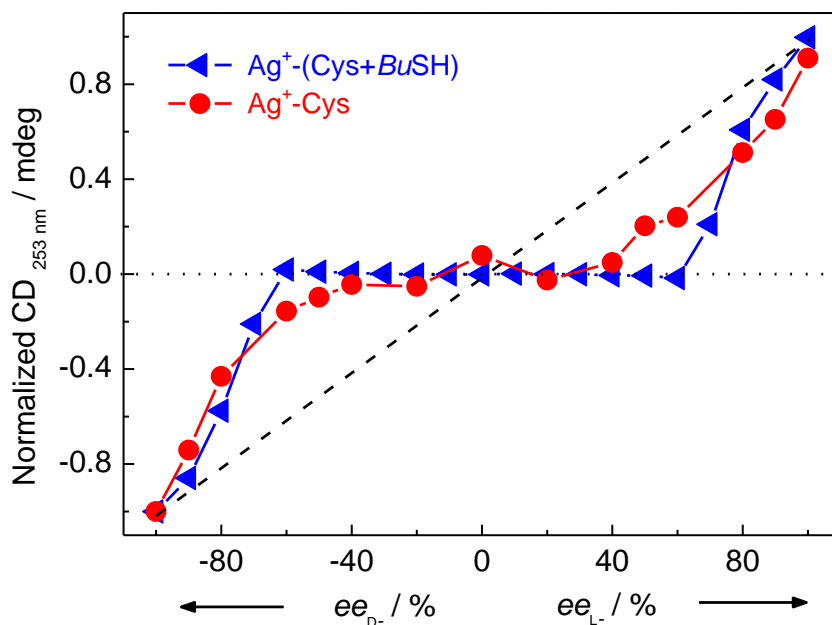
Fig. S34 Plots of normalized CD signals at 253 nm of Ag$^+$-(Cys+*Bu*SH) and Ag$^+$-Cys with varying *ee* of cysteine in 10 mM HAc-NaAc buffer of pH 5.0. [*Bu*SH] = 25 μM, [D-Cys] + [L-Cys] = 25 μM.
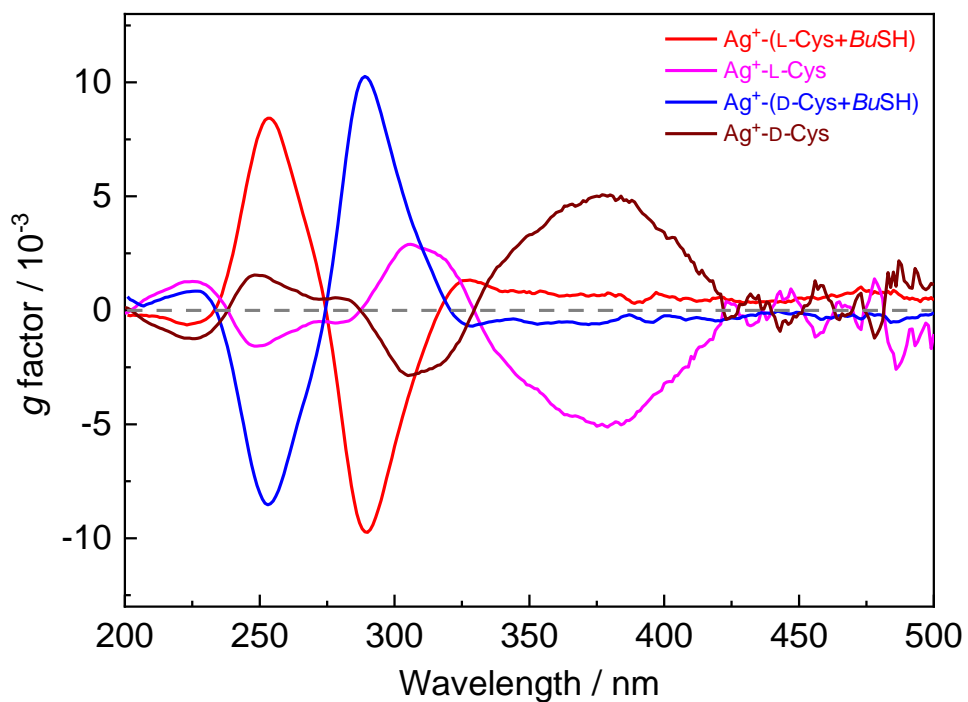
Fig. S35 The anisotropy factor *g* of Ag⁺-(L-/D-Cys+*Bu*SH) and Ag⁺-L-/D-Cys in 10 mM HAc-NaAc buffer of pH 5.0.

3. Supplementary Reference

1. H. J. Schöpe, O. Marnette, W. van Megen and G. Bryant, *Langmuir*, 2007, **23**, 11534.